Proton exchange membranes based on PVDF/SEBS blends

A. Mokrini *, M.A. Huneault

*Industrial Materials Institute, National Research Council of Canada, 75 de Mortagne Blvd.,
Boucherville, Que., Canada J4B 6Y4*

Abstract

Proton-conductive polymer membranes are used as an electrolyte in the so-called proton exchange membrane fuel cells. Current commercially available membranes are perfluorosulfonic acid polymers, a class of high-cost ionomers. This paper examines the potential of polymer blends, namely those of styrene–(ethylene-butylene)–styrene block copolymer (SEBS) and polyvinylidene fluoride (PVDF), in the proton exchange membrane application. SEBS/PVDF blends were prepared by twin-screw extrusion and the membranes were formed by calendering. SEBS is a phase-segregated material where the polystyrene blocks can be selectively functionalized offering high ionic conductivity, while PVDF insures good dimensional stability and chemical resistance to the films. Proton conductivity of the films was obtained by solid-state grafting of sulfonic acid moieties. The obtained membranes were characterized in terms of conductivity, ionic exchange capacity and water uptake. In addition, the membranes were characterized in terms of morphology, microstructure and thermo-mechanical properties to establish the blends morphology–property relationships. Modification of interfacial properties between SEBS and PVDF was found to be a key to optimize the blends performance. Addition of a methyl methacrylate–butyl acrylate–methyl methacrylate block copolymer (MMA–BA–MMA) was found to compatibilize the blend by reducing the segregation scale and improving the blend homogeneity. Mechanical resistance of the membranes was also improved through the addition of this compatibilizer. As little as 2 wt.% compatibilizer was sufficient for complete interfacial coverage and lead to improved mechanical properties. Compatibilized blend membranes also showed higher conductivities, 1.9×10^{-2} to $5.5 \times 10^{-3} \, \text{S cm}^{-1}$, and improved water management.
© 2005 Elsevier B.V. All rights reserved.

Keywords: Fuel cells; Proton exchange membrane; PVDF; SEBS; Melt blending; Compatibilization

1. Introduction

The proton exchange membrane (PEM) is a central component in polymer electrolyte membrane fuel cells (PEMFC). The major requirements for a PEM are high ionic conductivity, good mechanical strength and chemical resistance and low fuel permeability. Membrane materials are typically phase-segregated materials where a percolated network of a hydrophilic phase can conduct protons while the hydrophobic phase confers the mechanical strength and dimensional stability in the hydrated environment.

The current-state of the art proton exchange membranes are commercialized under the general Nafion tradename.

These are a family of perfluorosulfonic acid polymer membranes, which have a PTFE-like backbone with good physical characteristics for PEMFC. However, the cost of this material remains very high, added to the lack of selectivity for methanol of these membranes reduces drastically their performance when considering the development of direct methanol cells. In view of this, research efforts are focused on developing more economical alternatives based on partially fluorinated or non-perfluorinated polymer.

Partially fluorinated PEM can be made from synthesis of block copolymers where one of the blocks is a fluoropolymer. Recent publications have shown that it is possible to synthesize poly(arylene ethersulfone-*co*-vinylidene fluoride) block copolymer by polycondensation of α,ω-dihydroxy poly(arylene ethersulfone) precursors and α,ω-dibromo polyvinylidene fluoride [1,2], proton exchange membranes

* Corresponding author. Tel.: +1 450 641 5024; fax: +1 450 641 5105.
 E-mail address: Asmae.mokrini@cnrc-nrc.gc.ca (A. Mokrini).

are produced by sulfonation of resulting copolymer and casting from solution. Radiation grafting of reactive groups on perfluorinated base polymer is extensively used to produce partially fluorinated proton exchange membranes. Recently, polyvinylidene fluoride (PVDF) and poly(ethylene-tetrafluoroethylene) (ETFE) have been used as base polymer membrane, which has been irradiated with γ-ray or electron beam to produce activated polymer with radicals where a styrene-based monomer will be grafted and sulfonated [3–7]. Buchi et al. [3] have reported that partially fluorinated PEMs based on grafted polystyrene systems have physical and electrochemical properties superior than Nafion but an inferior performance in a H_2/O_2 fuel cell. They attributed this loss of performance to the excessive gas permeability of membranes that allow radical attack on the polystyrene grafts, but no proof was offered. However, Horsfall and Lovell [4] have demonstrated that sulfonated partially fluorinated PEMs based on styrene-grafted membranes have higher performance than Nafion in a H_2/O_2 fuel cell, but long-term testing shows a deterioration in performance compared to Nafion. The analysis of their MEA shows that the membrane maintained its properties and sulfonic acid content during fuel cell testing. Poor electrical contact between the membrane and the electrodes was found due to delamination of the MEA. This points to the need to adapt the MEA testing procedure developed for Nafion to the specific requirements of the alternative membrane materials.

Polymer blending is another potentially cost-effective route to achieve partially fluorinated PEMs. Development of membranes from thermo-plastic polymers by melt blending, could present a few key advantages over current solvent cast membranes. It offers a lower cost and solvent-free approach to large-scale membrane fabrication. The properties of these polymer blends are to a large extent determined by the blend morphology, which in turn depends on the processing history and on the interfacial properties. For most polymer blends, some interfacial modifications are necessary to get a finely dispersed and homogeneous blend and to insure the solid-state adhesion between the blend components. Compatibilization usually involves a third component that reduces the interfacial tension in the melt-state and improves the adhesion in the solid-state. This third component is ideally a block copolymer in which each of the blocks is entirely miscible in one of the blend components.

In this study, melt blending of polyvinylidene fluoride and of styrene–(ethylene-butylene)–styrene block copolymer (SEBS) was examined as a potential route toward phase-segregated materials suitable for membrane applications. PVDF, a semi-crystalline and chemically resistant polymer, is well suited to the fuel cells environment [8–9], and SEBS a phase-segregated material where the polystyrene block can be selectively functionalized offering high ionic conductivity [10–16]. Wnek and coworkers [12], obtained sulfonated SEBS (s-SEBS) by dissolving the polymer in a mixture of dichloroethane/cyclohexane, sul-

fur trioxide/triethyl phosphate sulfonating complex is then added, allowed to react 60–90 min below $0\,°C$. PEM are solvent cast from lower alcohols, with conductivities between 0.07 and $0.09\,S\,cm^{-1}$, when fully hydrated and depending on the degree of sulfonation. Other researchers carried out sulfonation in dichloroethane using acetyl sulfate as sulfonation agent [13,15], they obtain sulfonated polymers with higher thermo-oxidative stability than the unmodified polymer [13] and reduced methanol crossover [20]. PEMs based on s-SEBS are reported to be much less expensive to produce than Nafion, the main negative aspect in employing hydrocarbon-based materials is their poor oxidative stability compared to perfluorinated membranes [17,19], Ehrenberg et al. [18] suggest that their hydrocarbon nature require the development of electrodes which can be readily bonded to the membrane and enable an accurate evaluation of the performance.

In almost all the literature on s-SEBS, proton exchange membranes are prepared by casting from solution. Their morphology and physico-chemical behavior are expected to be much different from those of the extruded more crystalline form, and it is known that retention of a semi-crystalline morphology is important for mechanical strength and durability of polymer membranes. Therefore, melt blending of PVDF into SEBS may offer an interesting mean toward a chemically and mechanically stable proton conducting material. As a first step toward the membrane fabrication, this work will examine PVDF/SEBS blend morphology, microstructure and mechanical properties. A solvent-free sulfonation method will be used on extruded films to functionalize them and to provide proton conductivity. The ionic conduction, water uptake and ionic exchange capacity in functionalized polymer blend membranes will be discussed. In addition, the effect of a blend compatibilizer will be assessed.

2. Experimental

2.1. Materials

Polymers used were a styrene–(ethylene-butylene)–styrene triblock copolymer and polyvinylidene fluoride. The SEBS grade, G1652 supplied by Kraton Polymers contained 30 wt.% styrene and has an average molecular weight $M_w = 125,000$. The PVDF was Solef 1010 supplied by Solvay with $M_w = 77,000$. The copolymer used as compatibilizer is an experimental triblock copolymer of methyl methacrylate–butyl acrylate–methyl methacrylate (MMA–BA–MMA), supplied by Arkema Research. MMA–BA–MMA copolymer was used at levels of 2 and 10 wt.% based on the PVDF content. Chlorosulfonic acid, dichloroethane (DCE), dimethylacetamide (DMAc), methanol, sodium chloride, sodium hydroxide and phenolphthalein were purchased from Aldrich and used as received.

2.2. Membrane fabrication

SEBS/PVDF blends comprising 30, 40, 50 and 60 wt.% of PVDF were compounded on a 30 mm W&P co-rotating twin-screw extruder operated at a barrel temperature of 230 °C, a throughput of 5 kg h^{-1} and a screw speed of 150 rpm. The extruded strands were quenched in water, cut into granules and dried 24 h in an oven at 80 °C prior to film extrusion. The films were extruded at 230 °C and 100 rpm on a Randcastle laboratory cast film extrusion line. The extrusion die gap was set to 500 μm. The rolls temperature and speed were set to 70 °C and 0.5 cm min^{-1}, respectively, to achieve 200 μm thick films.

The films were immersed in a solution of chlorosulfonic acid (ClSO$_3$H) in 1,2-dichloroethane at room temperature to graft sulfonic moieties on the polystyrene blocks and provide proton exchange functionality. The ClSO$_3$H concentration was 0.75 M as this concentration was calculated to be high enough to maintain acid concentration constant during sulfonation. Sulfonation time was fixed to 60 min in order to compare the blends performance. The volume of the sulfonation solution was kept constant in relation to the mass of the film to be sulfonated. After sulfonation, membranes were first neutralized in methanol and then washed in distilled cold water until neutral pH, and in boiled water for 1 h. Sulfonated membranes were kept in deionized water for further analysis.

2.3. Blends and membrane characterization

For blend morphology analysis, strands extruded by the twin-screw extrusion process were microtomed perpendicular to the extrusion direction, and PVDF was extracted using DMAc as solvent. Scanning electron microscopy (SEM) was carried out on the Pt-sputtered surfaces at a 1 kV acceleration voltage. Fourier transform infrared (FTIR) spectroscopy was used to characterize samples. Due to their thickness (over 150 μm) and nature, some of the sulfonated films were practically opaque to IR. Therefore, attenuated total reflection (ATR) sampling technique was used for all the samples. Differential scanning calorimetry (DSC) was used to determine the thermal transitions of the blends. Samples were first cooled to −90 °C, and scanned from −90 to 250 °C to determine glass transition and melting temperatures, and from 250 to −90 °C to determine the crystallization temperature. The heating/cooling rate used was 20 °C min^{-1}. The crystallinity of PVDF in the samples was determined from the area under the melting peak, assuming a heat of fusion of $\Delta H_m^0 = 104.5 \, \text{J g}^{-1}$ for PVDF [21]. The tensile mechanical properties of films were measured according to standard ASTM D882. The test specimens consisted of strips 19 mm wide and 150 mm long. The gage length used was 50 mm. The samples were drawn at 500 mm min^{-1}. Each reported values are the average of five measurements.

Once the polymer films were functionalized with chlorosulfonic acid, their electrochemical properties were measured. First, ionic exchange capacity (IEC) was determined by soaking the membranes for 20 h in NaCl (0.2 M) and titrating them with NaOH (0.005 M) to the phenolphthalein end point. Sulfonation degree (SD) was calculated from IEC, and is defined as the ratio between sulfonated styrene repeating units and total styrene units. For water content determination, the samples were equilibrated in water at room temperature. They were then removed from the water container, quickly dry-wiped and immediately weighed. Subsequently, they were dried to weight constancy under vacuum at room temperature and again weighed. Then, the water content was calculated as follows: $((m_{\text{wet}} - m_{\text{dry}})/m_{\text{wet}}) \times 100$. Secondly, electrochemical impedance spectroscopy (EIS) was used to measure ionic conductivity of the membrane at ambient temperature and 100% relative humidity (RH). The impedance spectra were measured with an HP4192A impedance analyzer. For transverse and in-plane resistivity measurements, samples were sandwiched between blocking electrodes, and measured in deionized water (to simulate 100% RH). Scans were carried out in the 50 kHz–13 MHz frequency range with a 1 V applied ac signal. A Nafion 112 sample was measured as a reference before each series of measurements. As commonly accepted, the resistivity of a membrane was evaluated from the high frequency part of the Nyquist plot that coincides with the bulk resistance of the polymer. Ionic conductivity of the samples can be calculated by the following equation:

$$\rho = \frac{1}{R_b} \frac{d}{S}$$

where ρ is the conductivity ($\Omega^{-1} \, \text{cm}^{-1}$), d the distance between electrodes (cm), S the area electrodes contacting with the polymer film (cm^2) and R_b is the bulk resistance calculated from Nyquist plots (Ω).

3. Results and discussion

3.1. Blend morphology and compatibilization

In the first part of this study, the SEBS/PVDF blend morphology and the effect of a compatibilizing agent will be examined. In the current application, the membrane functionality depends on the SEBS material forming a continuous phase. The phase inversion point of the PVDF/SEBS blend is therefore of great interest to insure membrane functionality. However, in high viscosity fluids such as polymer melts, the phase inversion is not a sharp transition. Instead, there is certain concentration range, typically in the 40–60 vol% range, where we have the so-called co-continuous morphology where both phases form an interconnected continuous network. It is possible to increase the volume fraction at which phase inversion or co-continuity occurs by increasing the viscosity of the dispersed component relative to that of the matrix phase. For the membrane application, continuity of the SEBS phase is necessary to yield proton conductivity in the sulfonated-state. Therefore, the PVDF must form
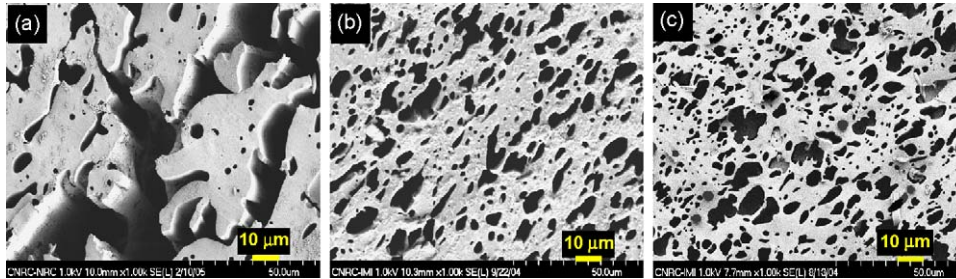
Fig. 1. SEM micrographs on microtomed strands of SEBS/PVDF (50:50 wt.%) blends, after PVDF extraction (a) without compatibilizer, (b) with 2 wt.% MMA–BA–MMA block copolymer and (c) with 10 wt.% MMA–BA–MMA block copolymer.

either a dispersed or co-continuous morphology to maintain functionality of the material. The 30–60 wt.% PVDF used in this study correspond on a volume basis to 18–43 vol%. Since the viscosity of PVDF and SEBS are relatively well matched at the processing deformation rates, it is expected that PVDF will be the dispersed phase in the range of compositions studied. During blend extrusion and film forming processes, these PVDF domains, even at low PVDF concentrations, are deformed into elongated structures or fibers and interconnected in the matrix, leading to self-reinforcing polymer blends.

SEBS and PVDF are immiscible polymers with a high interfacial tension, leading to poor dispersion and interfacial adhesion. A triblock copolymer of MMA–BA–MMA was evaluated as compatibilizer. The MMA blocks are known to be miscible with PVDF while the olefinic derivatives have low interfacial tensions with the olefinic blocks of SEBS. Fig. 1 shows SEM micrographs of microtomed strands of SEBS/PVDF (50:50 wt.%) blends, after PVDF extraction without compatibilizer and with two concentrations of MMA–BA–MMA block copolymer. Clear changes are observed when 2 wt.% of MMA–BA–MMA is added, co-continuous morphology observed for the non-compatibilized blend break up into dispersed morphology, accompanied by an important phase size reduction. This indicates that it is decreasing the interfacial tension between PVDF and SEBS in the blend. No significant improvement is observed for higher concentration, 2 wt.% is sufficient for complete interfacial coverage. The block copolymer was therefore used as a compatibilizer for further blends.

In order to determine possible interactions or changes due to blending and compatibilization, FTIR digital absorbance subtractions technique was used. We used characteristic C=O stretching frequency of the PMMA at $1729 \, cm^{-1}$ to determine the correct subtraction parameter of compatibilizing agent spectrum from that of the blend, and characteristic frequency of SEBS at 698, 2852 and $2922 \, cm^{-1}$. Fig. 2 shows the ATR spectra of pure PVDF and those of the PVDF present in the 40 wt.% PVDF blends with different compatibilizer concentrations. Those have been determined from the blend spectra after subtraction of the SEBS and MMA–BA–MMA absorption bands. The first observation is the shift of the band at $871.5 \, cm^{-1}$ in pure PVDF, to $873 \, cm^{-1}$ in the blends. This absorption band corresponds to the crystalline phase in pure PVDF (α, β or γ) [22]. The shift is due to the presence of SEBS, however the crystalline content of the PVDF remains constant around 60%, and independent of SEBS concentration of the blends as will be seen in DSC.

The spectra of PVDF extracted from the blends with different compatibilizer content, are basically the same, which suggests that the majority of the PVDF is unaffected by the presence of the MMA functionality of compatibilizer, except for the absorption band at $844 \, cm^{-1}$ that shifts and decreases with increasing compatibilizer concentration as can be seen in Fig. 3. This band is characteristic of the C–H rocking vibration in the CH_2 groups of PVDF [23]. Furthermore, in compatible PMMA/PVDF blends, it is known that attractive intermolecular interactions (hydrogen bond) take place between PMMA carbonyl group and PVDF hydrogen atoms which explains the changes observed, that suggest some small but distinct interaction involving CH_2 group of PVDF [24].

The SEBS and PVDF blends are immiscible and as expected the glass transition and melting temperatures were found to be insensitive to blend composition in the range of concentration studied. Fig. 3 presents the crystalline content of the PVDF in the blends. The crystalline content for the PVDF/SEBS is constant with PVDF concentration within experimental errors. However, in the case where 2 and
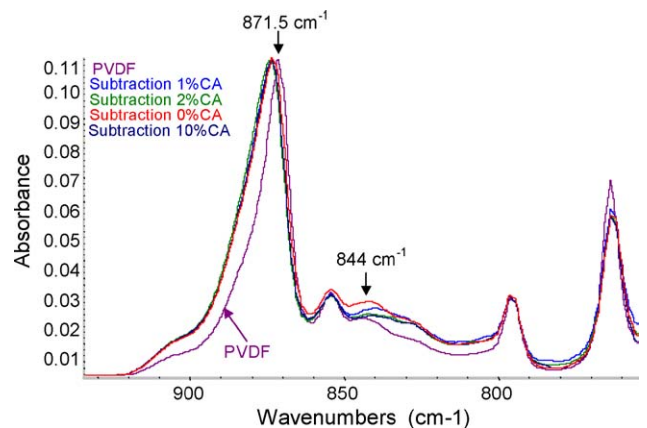

Fig. 2. FTIR spectra of pure PVDF and those of the PVDF present in the 40 wt.% PVDF blends with different compatibilizer concentrations after subtraction of the SEBS and MMA–BA–MMA absorption bands.
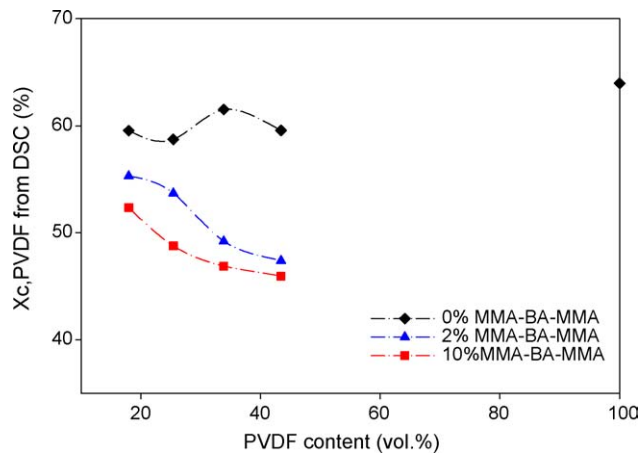
Fig. 3. Crystalline fraction of PVDF in SEBS/PVDF blends with different concentrations of MMA–BA–MMA block copolymer as measured from DSC analysis.

10 wt.% of the triblock copolymer is added, the crystalline content decreases from 60 to 45% approximately. This is due to the disruption of the PVDF crystalline network by the miscible but non-crystallisable PMMA blocks of the triblock MMA–BA–MMA copolymer as has been observed by others [25].

3.2. Mechanical properties

When blending a low modulus elastomer with a stiffer PVDF material, the resulting properties will be very sensitive to the blend composition, morphology and interfacial properties. Figs. 4 and 5 present the tensile modulus and strain at break of blend membranes as a function of the PVDF content, respectively. At low PVDF concentration (e.g. 0–20 vol%), small-dispersed droplets are expected to act as particulate filler while at higher concentration; the PVDF may act as fiber reinforcement.

The tensile modulus, presented in Fig. 4, increases rapidly with the PVDF content as we are typically in a fiber–matrix blend composition range. Since the film casting and calendaring induced more machine direction (MD) stretching, we have a preferential PVDF fiber orientation in the MD direction, which translates into much a higher MD than TD modulus.

Conversely, the strain at break decreases with PVDF concentration as expected from the stiffening of the material combined with the relatively poor solid-state adhesion of the blend components.

Since the modulus is measured at the initial deformation, it is not expected to be sensitive to interfacial adhesion. Nonetheless, the addition of the triblock MMA–BA–MMA compatibilizer causes a slight increase in MD tensile modulus but has little or no effect in the TD. This can be associated to increased fibrillar content or to the intrinsically higher modulus of the copolymer compared to the SEBS matrix. Clearly, this effect is more pronounced in the presence of high ori-
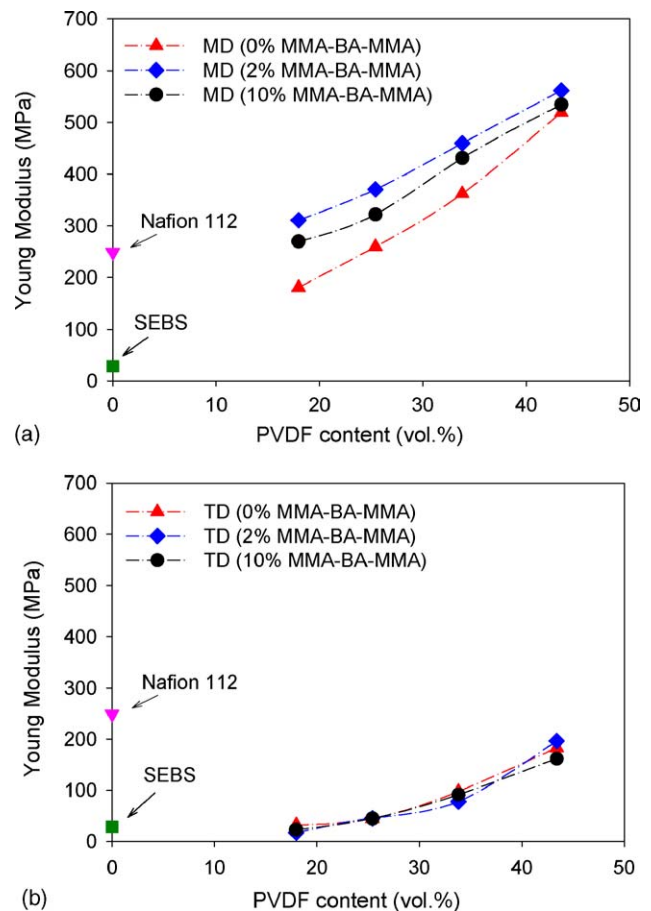

Fig. 4. Young modulus of SEBS/PVDF blend membranes with different concentrations of MMA–BA–MMA block copolymer in: (a) machine direction and (b) transverse direction.

entation. The compatibilizer plays a more important role on the strain at break. The highest elongation is obtained with 2 wt.% of triblock copolymer. That suggests that this concentration is sufficient for complete interfacial coverage. Further addition probably results in micelles that do not contribute to the interface modification.

3.3. Characterization of functionalized membranes

In the third part of this study, we will evaluate how sulfonation kinetics and properties of sulfonated SEBS vary with blending and compatibilization. Blend membranes were functionalized according to the procedure described in Section 2.

Fig. 6 compares a series of ATR spectra for a 40 wt.% PVDF/SEBS blend before (1) and after sulfonation (2). The arrows denote the positions of the new bands that result from the sulfonation reaction. The absorbance at $1006.6\,cm^{-1}$ results from the in-plane bending vibration of phenyl ring substituted with a sulfonate group and the $1034.6\,cm^{-1}$ is due to the symmetric stretching vibration of the sulfonate group. The absorbance at $1126.94\,cm^{-1}$ results from sulfonate anion
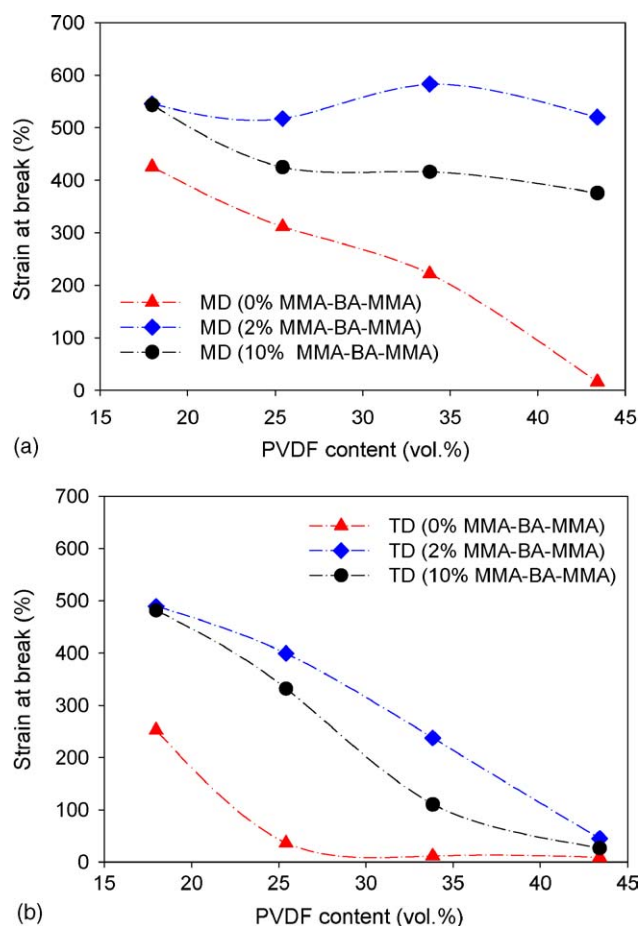
Fig. 5. Strain at break of SEBS/PVDF blend membranes with different concentrations of compatibilizer: (a) MD and (b) TD.

attached to phenyl ring. An increase in the intensity of the large band between 1650 and 1800 cm^{-1} characteristic of the combination vibrations (finger bands) of phenyl group, is also observed. The spectra of a sulfonated blend (also containing 40 wt.% PVDF) that was compatibilized with 2 wt.% MMA–BA–MMA is shown as curve 3. No new bands were observed compared to the uncompatibilized blend. However, the new absorption bands that appeared upon sulfonation show increased intensities for the compatibilized blend. The increase in intensity (relative to the amount of sulfonation) could be associated to the change in blends morphology after compatibilization observed with SEM analysis, where the dispersed morphology of PVDF domains facilitates attachment of acid functionality.

In sulfonic acid-based membranes, the proton conductivity depends on the number of available acid groups and their dissociation capability in water. When the membrane is in the hydrated form, water molecules dissociate acid functionality and facilitate proton transport. Therefore, the conductivity and ionic exchange capacity are important parameters in studying PEMs. Swelling is also a key factor for the mechanical integrity of the membranes. Excessively high levels of water can result in dimensional changes leading to failures in mechanical properties. All these parameters have been determined for the series of membranes studied and are reported in Table 1. PVDF content was varied from 30 to 60 wt.%, for fixed compatibilizer content of 0, 2 and 10 wt.% based on the PVDF content. The results are compared to s-SEBS and Nafion 112.

In order to extract meaningful relations between results within a series of samples and between series, conductivity,
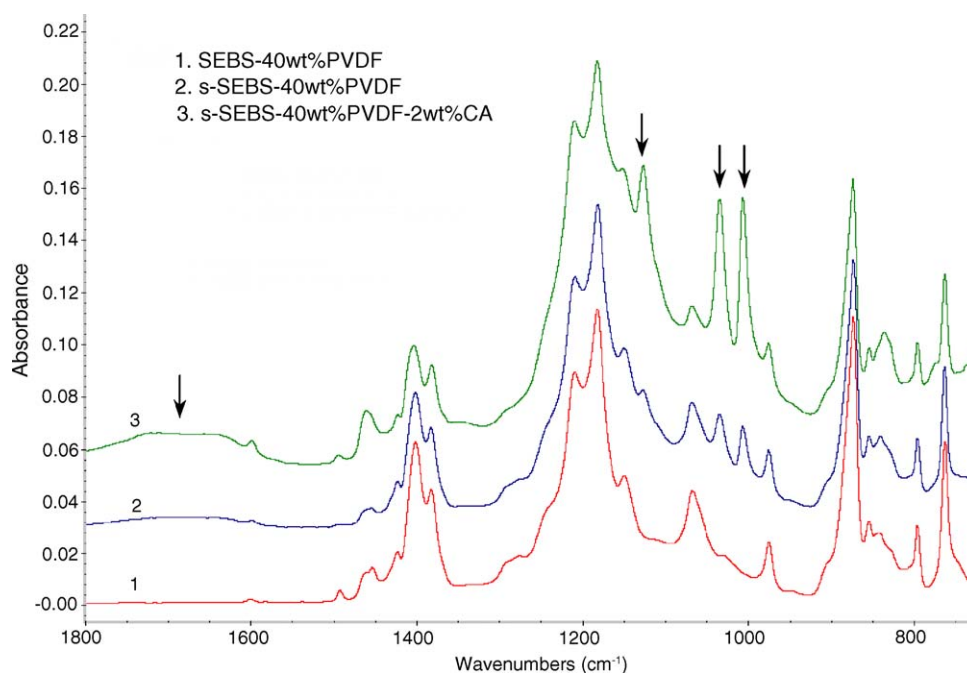

Fig. 6. FTIR spectra of: (1) SEBS/PVDF blend with 40 wt.%PVDF; (2) sulfonated blend; (3) sulfonated compatibilized blend (with 2 wt.% MMA–BA–MMA).

Table 1
Properties of sulfonated SEBS/PVDF polymer blend membranes with 0, 2 and 10 wt.% MMA–BA–MMA compatibilizer

Sample	SEBS (wt.%)	CA[a]/PVDF (wt.%)	DS (%)	IEC (titrating) (meq g^{-1})	Water content (%)	(H$_2$O)/(SO$_3{}^-$)	Conductivity (S cm^{-1})
Nafion 112	–	–	–	0.74	22.54	16.95	2.04E−02
s-SEBS	0	0	33.39	1.80	60.79	18.73	3.55E−02
s-SEBS/PVDF	40	0	10.87	0.59	54.65	51.75	1.99E−04
s-SEBS/PVDF	50	0	14.90	0.80	56.53	39.04	2.06E−03
s-SEBS/PVDF	60	0	17.81	0.96	60.67	35.05	6.73E−03
s-SEBS/PVDF	70	0	19.44	1.05	58.97	31.21	1.25E−02
s-SEBS/PVDF/CA	39.5	2	13.16	0.71	58.71	45.90	7.37E−04
s-SEBS/PVDF/CA	49.5	2	17.56	0.95	64.80	37.97	6.43E−03
s-SEBS/PVDF/CA	59.5	2	21.63	1.17	64.59	30.71	1.32E−02
s-SEBS/PVDF/CA	69.6	2	24.99	1.35	62.79	25.84	1.71E−02
s-SEBS/PVDF/CA	37.7	10	16.07	0.87	63.31	40.53	5.50E−03
s-SEBS/PVDF/CA	47.6	10	19.64	1.06	71.05	37.23	1.07E−02
s-SEBS/PVDF/CA	57.7	10	23.28	1.26	71.23	31.47	1.60E−02
s-SEBS/PVDF/CA	68.0	10	26.52	1.43	65.27	25.21	1.94E−02

[a] CA: compatibilization agent MMA–BA–MMA block copolymer.

IEC and (H$_2$O)/(SO$_3{}^-$) ratio were considered. Fig. 7a plots the conductivity of the membranes as a function of IEC. In general, the blends exhibited lower ionic exchange capacity and conductivity than s-SEBS as expected. IEC was 1.8 meq g^{-1} for s-SEBS (corresponding to a degree of sulfonation DS of 33.4%), and ranges from 0.6 to 1.5 meq g^{-1} (DS from 10.8 to 26.5%) for the blend membranes. Within a series, the overall increase in IEC with increasing s-SEBS content is consistent with a highest sulfonic acid content and highest degree of sulfonation, considering that PVDF is inert to sulfonation and all conduction occurs through sulfonic acid groups grafted in styrene blocks of SEBS. If we compare series, the conductivity varies between 2.0×10^{-4} and 1.3×10^{-2} S cm^{-1} for sulfonated PVDF/SEBS series, and 5.5×10^{-3} and 1.9×10^{-2} S cm^{-1} when 10 wt.% MMA–BA–MMA copolymer was added. This increase in conductivity and IEC is related to the morphological changes observed due to compatibilizing effect of MMA–BA–MMA block copolymer. Co-continuous morphology observed for the non-compatibilized blend break up into dispersed morphology, accompanied by an important phase size reduction in PVDF domains that favors functionalization reaction of SEBS.

Fig. 7b plots the conductivity of the membranes as a function of (H$_2$O)/(SO$_3{}^-$) ratio. The (H$_2$O)/(SO$_3{}^-$) ratio for a water-swollen membrane describes the number of water molecules per fixed ion sites and is equivalent to the ratio of water molecules to protons. Comparison of this ratio for different membranes allows for a qualitative comparison of the fraction of free water present within the membranes.

Within a series, the highest (H$_2$O)/(SO$_3{}^-$) ratio is observed for membranes with the highest PVDF content and lowest conductivity as can be seen in Fig. 7b. This translates into a higher fraction of free water for samples with higher PVDF content. To explain such high values, morphology
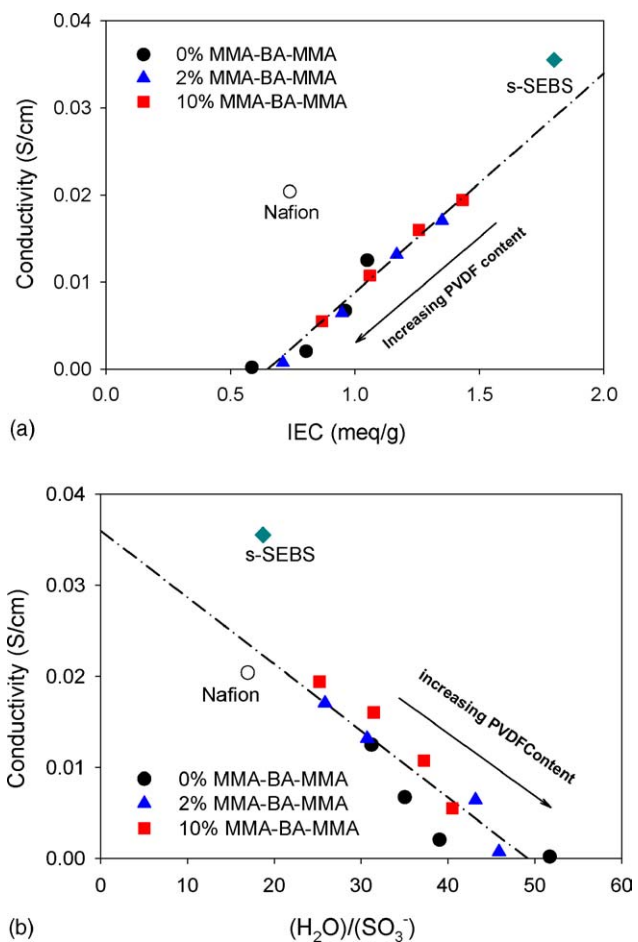

(a)

(b)

Fig. 7. Transverse conductivity as a function of: (a) IEC and (b) (H$_2$O)/(SO$_3{}^-$) for s-SEBS/PVDF blends with different compatibilizer contents (sulfonation time = 1 h).

of these blends should be considered. At low PVDF content, PVDF is dispersed as particulate filler in a continuous SEBS matrix, while for higher content, PVDF domains are interconnected in a more continuous network. Furthermore, if we consider the poor solid-state interfacial adhesion due to the immiscibility of SEBS and PVDF, and dimensional changes that involve SEBS phase after sulfonation, leads to an increase in free water content in the membranes. A diminution of the $(H_2O)/(SO_3^-)$ ratio is observed for series where MMA–BA–MMA block copolymer is incorporated to the blends (Fig. 7b), since its compatibilization effect improves phase dispersion in blend membranes by reducing phase size of PVDF domains and enhances connectivity and adhesion. In turn, this enhances overall membranes properties.

4. Conclusions

Partially fluorinated membranes based on SEBS and PVDF blends have been produced by extrusion in the melt-state and films produced by calendaring technology. The phase-segregated materials exhibited relatively good mechanical properties. Proton conductivity was obtained by successfully grafting sulfonic acid groups on the styrene blocks of SEBS in the pre-formed films. The reported conductivity is in an acceptable range for proton exchange membranes applications, and can be varied through changes in blend composition. The membranes with lower PVDF content, exhibit higher conductivity but lower mechanical properties, conversely to the membranes with high PVDF content. Compatibilization of a SEBS/PVDF blend is reported for the first time in this paper, with the use of a triblock copolymer of methyl methacrylate and butyl acrylate (MMA–BA–MMA). It was shown that the incorporation of concentration as low as 2 wt.% decreases the segregation scale leading to superior mechanical properties; it also improves conductivity and enhances water management in functionalized samples. The $(H_2O)/(SO_3^-)$ ratio was very high even in compatibilized blends however. This is probably due to the presence of free water at the blends interface. This could be reduced by further improving the interfacial adhesion between PVDF and SEBS and will be addressed in future work. Finally, it is noteworthy that the low methanol permeability of the studied materials makes the developed membranes particularly appropriate for direct methanol fuel cells. Performance of these membranes in direct methanol fuel cell is under study.

References

[1] Y. Yang, Z. Shi, S. Holdcroft, Eur. Polym. J 40 (2004) 531.
[2] Y. Yang, Z. Shi, S. Holdcroft, Macromolecules 37 (2004) 1678.
[3] F.N. Buchi, B. Gupta, O. Haas, G.G. Scherer, Electrochim. Acta 40 (1995) 345.
[4] J.A. Horsfall, K.V. Lovell, Fuel Cells 1 (2001) 186.
[5] S.D. Flint, R.C.T. Slade, Solid State Ionics 97 (1997) 299.
[6] M. Shen, S. Roy, J.W. Kuhlmann, K. Scott, K. Lovell, J.A. Horsfall, J. Membr. Sci. 251 (2005) 121.
[7] M. Asukabe, M. Kato, T. Taniguchi, Y. Morimoto, M. Kawasumi, US Patent 6,827,986 (2004).
[8] B. Soresi, E. Quartarone, P. Mutarelli, A. Magistris, G. Chiodelli, Solid State Ionics 166 (2004) 383.
[9] Y. Si, J.C. Lin, H.R. Kunz, J.M. Fenton, J. Electrochem. Soc. 151 (3) (2004) 463.
[10] D.E. Winkler, US Patent 3,577,357 (1971).
[11] B.M. Sheikh-Ali, G.E. Wnek, US Patent 6,11,616 (2000).
[12] S.G. Ehrenberg, J.K. Serpico, G.E. Wnek, J.N. Rider, US Patent 5,468,574 (1995).
[13] R.A. Weiss, A. Sen, C.L. Willis, L.A. Pottick, Polymer 32 (10) (1991) 1867.
[14] G.E. Wnek, J.N. Rider, J.M. Serpico, A.G. Einset, Electrochemical Society Proceedings of the First International Symposium on Proton Conducting Membrane Fuel Cells, 1995, p. 247.
[15] A. Mokrini, J.L. Acosta, Polymer 42 (2001) 9.
[16] C.A. Edmondson, J.J. Fontanella, S.H. Chung, S.G. Greenbaum, G.E. Wnek, Electrochim. Acta 46 (2001) 1623.
[17] R.B. Hodgdon Jr., J. Polym. Sci. 6 (1968) 171.
[18] S.G. Ehrenberg, J.M. Serpico, B.M. Sheikh-Ali, T.N. Tangredi, E. Zador, G.E. Wnek, Proceedings of the Second International Symposium on New Materials for Fuel Cell and Modern Battery Systems, 1997, p. 828.
[19] V.I. Basura, C. Chuy, P.D. Beattie, S. Holdcroft, J. Electroanal. Chem. 501 (2001) 77.
[20] A. Mokrini, J.L. Acosta, Proceedings of the Fourth International Symposium on New Materials for Electrochemical Systems, 2001, p. 365.
[21] K. Nakagawa, Y. Ishida, J. Polym. Sci.: Polym. Phys. Ed. 11 (1973) 2153.
[22] Y. Bormashenko, R. Pogreb, O. Stanecsky, E. Bormashenko, Polym. Testing 23 (2004) 791.
[23] L.K. Yoon, B.K. Kim, J. Appl. Polym. Sci. 78 (2000) 1374.
[24] D. Jouannet, T.N. Pham, S. Pimbert, G. Levesque, Polymer 38 (20) (1997) 5137.
[25] T. Nishi, T.T. Wang, Macromolecules 8 (1975) 909.